Spin observables in 71*A* MeV ^{6,8}He-hydrogen scattering

S. Karataglidis* and K. Amos†
Department of Physics, University of Johannesburg, P.O. Box 524, Auckland Park, 2006, South Africa and School of Physics, The University of Melbourne, Victoria 3010, Australia
(Received 7 May 2013; published 31 May 2013)

Predictions of cross sections and analyzing powers using g-folding optical potentials for the scattering of 71A MeV ^{6,8}He ions from (polarized) hydrogen are compared with data. A g-folding model in which exchange amplitudes are evaluated explicitly was used with wave functions of ^{6,8}He specified from a no-core shell model that used a complete $(0+2+4)\hbar\omega$ basis. The analyzing powers reveal some sensitivities to the details of the wave functions, especially in the case of halo nuclei.

DOI: 10.1103/PhysRevC.87.054623 PACS number(s): 25.40.Cm, 21.10.Gv, 21.60.Cs, 24.10.Ht

I. INTRODUCTION

It has been possible, for quite some time, to make predictions of nucleon-nucleus (*NA*), elastic scattering observables [1], and, under a distorted wave approximation (DWA), predictions also of observables from inelastic scattering and charge exchange reactions. Such analyses have been possible using a completely microscopic formulation of scattering [1]. As all details required in the calculations are preset, with no adjustable parameters, the results of these calculations are predictions of the relevant scattering observables. Only one run of the scattering code (DWBA98 [2] in our case) is needed. Complete details as well as many examples of use of this (coordinate space) microscopic model approach are to be found in the review [1]. Use of the complex, nonlocal, nucleon-nucleus optical potentials defined in that way predicted cross sections and spin observables in good agreement with data from many stable nuclei (^{3}He to ^{238}U) and for a wide range of energies (25 to 300 MeV). Crucial to that success was use of effective nucleon-nucleon (*NN*) interactions built upon *NN*g matrices that are solutions of Brueckner-Bethe-Goldstone (BBG) equations for realistic starting free *NN* interactions. The effective *NN* interactions are complex, energy, and density dependent, have central, two-nucleon tensor and two-nucleon spin-orbit character, with each component represented by a form factor formed as a mixture of Yukawa functions. Details of this Melbourne force are also given in the review [1]. The *NA* optical potentials result from folding those effective interactions with the one-body (ground) state density matrices (OBDME) of the target nucleus, as obtained from a suitable model of structure with nucleonic degrees of freedom.

Antisymmetrization of the projectile with all target nucleons leads to exchange (knock-out) amplitudes, so making the microscopic optical potential nonlocal. An important facet is that nonlocality should be treated explicitly in the calculations of scattering. For brevity, the optical potentials that result are called g-folding potentials.

The level of agreement found between predictions of scattering observables made using the g-folding potentials has been excellent for stable nuclei across the mass range. This is particularly true for the analyzing powers at 65 and 200 MeV [1], where, at 65 MeV, the zero analyzing power to large angles, and subsequent structures, have been reproduced for all nuclei from mass-7 to mass-238. (See Figs. 10.3 and 10.4 of Ref. [1].) It is also noteworthy that the model has been applied to the scattering of exotic nuclei from hydrogen [3–6] with equal success. Another application has been the prediction of integral observables of elastic scattering, for both protons and neutrons, with quite good agreement [7]. Thus, the method is known to give good predictions of angular-dependent and integral observables, which is not guaranteed when the usual phenomenological approaches are used.

Of importance, however, is that the level of agreement with data in the g-folding approach depends on the quality of what is used for the underlying model of structure. Due to the character of the hadron force, proton scattering is preferentially sensitive to the neutron matter distributions of nuclei: a sensitivity seen in a recent assessment, using proton elastic scattering, of diverse Skyrme-Hartree-Fock model structures for ^{208}Pb [8]. Such is the breadth of success with target mass and varied energies that the effective *NN* interactions have been established, and so new predictions of nucleon scattering can be considered as a test of the quality of the assumed nuclear structure.

Note that g-folding theory of *NA* elastic scattering (and in the DWA, of inelastic and charge exchange reactions) involves three preset quantities. They are

(i) an effective *NN* interaction,
(ii) the one body density matrix elements (target structure information), and
(iii) the target single-nucleon bound state wave functions.

Once specified, a single calculation of scattering suffices to obtain a prediction. The effective interaction for 71 MeV incident protons has been formed as is specified in the review [1]. Nonetheless a brief review is given next to allow interpretation of results of the analyses of ^{6,8}He ions scattering from hydrogen. Details of the structures used are presented in the following section, and the results of analyses of the 71A MeV data [9] are given thereafter.

II. THE EFFECTIVE INTERACTION

A realistic microscopic model of *NA* reactions is taken to be one that is based upon *NN* interactions whose on-shell values

*stevenka@uj.ac.za
†amos@physics.unimelb.edu.au

of t matrices (solutions of Lippmann-Schwinger equations) are consistent with measured NN scattering data up to the chosen limit energy of 300 MeV. Below pion threshold, the phenomenology of the NN interaction is relatively simple, and several one-boson-exchange potential models exist with which very good fits have been found to NN phase-shift data.

But the presence of the nuclear medium alters such pairwise interactions between an incoming (positive energy) nucleon and any (bound) nucleon in the target from the free NN scattering case. The result is an effective NN interaction. For incident proton energies to 300 MeV, it is useful to choose that effective interaction to be a mix of central, two-body spin-orbit, and tensor forces, each having a form factor that is a sum of Yukawa functions. Each of those functions has a complex, energy, and density dependent strength. The ranges and strengths are obtained by accurately mapping the double Bessel transform of the effective interaction to the (NN) g matrices of the Bonn-B potential. Those g matrices are the solutions of the BBG equations, in momentum space, for energy $E \rightarrow k^2$ and for diverse Fermi momenta, k_F,

$$
\begin{aligned}
&g^{JST}_{LL'}(p, p'; k, K, k_F) \\
&\quad = V^{JST}_{LL'}(p, p') + \frac{2}{\pi} \sum_l \int_0^\alpha V^{JST}_{Ll}(p', q) \\
&\qquad \times \left[\frac{\bar{Q}(q, K, k_F)}{\bar{E}(k, K, k_F) - \bar{E}(q, K, k_F) + i\varepsilon} \right] \\
&\qquad \times g^{JST}_{lL'}(q, p; k, K, k_F)\, q^2 dq, \qquad (1)
\end{aligned}
$$

in which $\bar{Q}(q, K, k_F)$ is an angle-averaged Pauli operator and $\bar{E}$ are single particle energies, all evaluated at an average center-of-mass momentum, K. The energy and density dependence of the complex effective NN interactions so formed have been crucial in forming the optical potentials that yield good predictions to measured data at many energies and from many target nuclei [1]. One may also consider the extension of the angle-averaged Pauli operator to the nonspherical case [10]. The issue is to consider properly the G-matrix elements from the tensor interaction, and how it may affect non-natural parity transitions in inelastic scattering. But a study of the inelastic scattering to the 4^- states in ^{16}O [11], or to the 10^- state in ^{208}Pb [12], using the Melbourne g-folding model, found no such problems.

To illustrate the propriety of this form of effective NN interaction as well as of the credibility of the g-folding approach, cross sections for the scattering of ^{6}He ions from Hydrogen are shown as functions of momentum transfer in Fig. 1. The g-folding (and DWA for the inelastic scattering) results are compared with data taken at 40.9A MeV [5] (displayed by the open circles) and at 24.5A MeV [6] (displayed by the filled squares). Elastic scattering data are shown in the top segment and inelastic scattering data from the excitation of the 2^+_1 (1.8 MeV) state are shown in the bottom segment. The solid and dashed curves are the results of predictions of the 40.9A MeV and of the 24.5A MeV data, respectively, made assuming that ^{6}He has a neutron halo. The inelastic scattering results were obtained using the (predictive) DWA approach in which the distorted waves were generated from the g-folding optical potentials with which

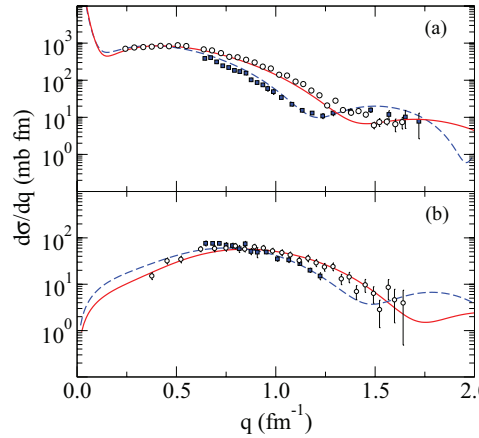

FIG. 1. (Color online) (a) Elastic and (b) inelastic differential cross sections for ^{6}He scattering from hydrogen. Data and curves are identified in the text.

the elastic scattering cross sections were well reproduced and the transition OBDME were obtained from the no-core shell model calculation that also gave the ground state OBDME. The same Woods-Saxon (WS) bound state functions that gave a neutron halo and lead to the good cross sections for elastic scattering were also used as the single-particle (SP) wave functions for both the ground and excited state. The effective NN interaction used to form the g-folding optical potentials was also used as the transition operator effecting the inelastic scattering. Consequently all details describing the inelastic excitation within the DWA have been preset so that inelastic scattering magnitudes, in particular, are predictions. No core polarization, or other scaling values, are needed to obtain agreement with data. In fact, it is the magnitude of the forward scattering angle (low momentum transfer) inelastic cross section data that is prime evidence of the neutron halo properties of the ^{6}He states [5,6]. That the overall (shell model) approach is valid is confirmed by the self-consistent and predictive descriptions of the elastic, inelastic, and reaction cross sections [5]. The transition form factor for inelastic scattering stresses the properties of the nuclear surface and, consistent with that, extension of the neutron matter influences low momentum transfer aspects of that scattering. In contrast, and as shown by the lower energy results [5,6], the neutron halo effects in the elastic scattering cross sections are most evident at momentum transfer values greater than $\sim$1 fm^{-1}. This reflects the influence of the bulk volume properties of the ^{6}He wave functions in defining the optical potentials: it is the depletion of neutron density in the inner region, coming from the extension of the neutron density at the surface to large radii, that results in the reduction of the differential cross section at large momentum transfers.

As the same structure (OBDME, SP wave functions, etc.) was used in the calculations at both energies, the results plotted here as functions of momentum transfer not only confirm the neutron-halo character of ^{6}He but also reveal that the effective interaction varies radically with energy and density in a way well defined by the BBG approach to its definition. Thus predictions for the scattering at 71A MeV can be expected to have high probability of matching data. Indeed the predicted

cross section does match existing cross-section data [13] as will be shown again later. The new data, for analyzing powers [9] are considered now since those are very sensitive to details of the scattering matrices. One might expect predictions of the analyzing power at 71A MeV to be realistic since very good agreement has been found with g-folding model predictions spin observables with data from the scattering of 65 and 200 MeV protons from many stable nuclei [1]. However, spin observables are very sensitive to details in scattering theory, with analyzing powers in particular being so on specifics of structure [1].

III. STRUCTURE OF ^{6,8}HE

^{6}He and ^{8}He are among the most studied of the exotic systems given that they lie close to both the valley of stability and the neutron drip line. They are Borromean since ^{5,7}He are both neutron-unstable. ^{6}He is classed as a two-neutron halo nucleus, though the term is perhaps unfortunate: rather, it should be viewed as a nucleus with an exceptionally extended neutron density. ^{8}He is not a neutron-halo nucleus: it is a neutron-skin nucleus. Both descriptions are supported by analyses of existing proton scattering data [4,5].

For the purposes of the present study, a complete $(0+2+4)\hbar\omega$ shell model has been used [4] to describe both ^{6}He and ^{8}He. The Zheng [14] G-matrix shell model interaction, as derived from the Nijmegen III NN interaction [15], was used to define the Hamiltonians. The structures so defined not only provide the OBDME (or occupation numbers) defining the density in the case of elastic scattering and transition OBDME for inelastic scattering but also the relevant SP wave functions. The Zheng G-matrix interaction requires a specification of the oscillator energy to obtain the two-body potential energy matrix elements so that energy specifies the oscillator parameter for use in the scattering calculations. We have used $\hbar\omega = 14$ MeV in the $(0+2+4)\hbar\omega$ space calculations. But all such shell model wave functions do not give a neutron-halo character. At best, and due to the Gaussian SP functions involved, the density profiles from the shell model information form neutron (proton) skins.

In the case of ^{6}He, established now as a halo nucleus [5], oscillators need be replaced with, for example, WS wave functions to effect an extended neutron matter character. (This was necessary to reproduce the $B(E1)$ value in ^{11}Be [16].) By choosing the binding energy of the halo-neutron orbits to be fixed by the single neutron separation energy to the lowest energy resonance in ^{5}He (1.8 MeV), the associated density profile has the extensive neutron density that is characterized as a halo. To date that has sufficed to replicate cross section data for many incident ion energies, even at 15A [17] with ^{8}He, where the use of WS functions describes well the skin of ^{8}He.

IV. DIFFERENTIAL CROSS SECTIONS AND ANALYZING POWERS

g-folding model results (of elastic scattering) are pertinent for calculated differential cross sections exceeding a few tenths of a mb/sr. Typically that range for 71 MeV protons reaches 100° to 110° in the center of mass.

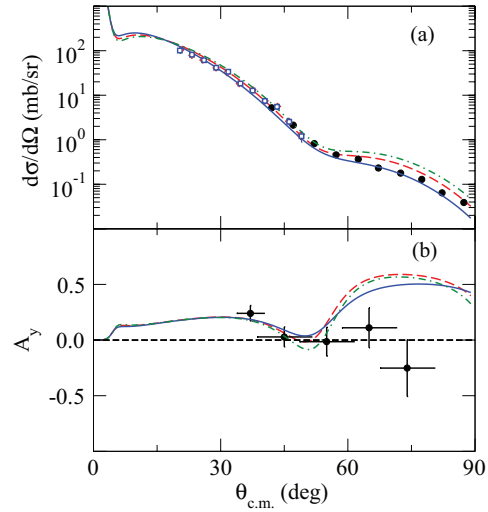

FIG. 2. (Color online) (a) Differential cross sections and (b) analyzing powers for the scattering of 71A MeV ^{6}He ions from hydrogen. The halo, no halo, and oscillator ($b = 1.7$ fm), are portrayed by the solid, dashed, and dot-dashed lines, respectively.

The differential cross sections and analyzing powers for the elastic scattering of ^{6}He ions from hydrogen are shown in Fig. 2. The results of three calculations are presented, the difference is in the choice of single particle wave functions used. The solid line is the result using the WS set as in Fig. 1, while the dashed and dot-dashed lines show the results of the calculations made using WS functions with a larger binding energy (∼7 MeV) for the neutrons in the $0p$ shell (hereafter known as the "no halo" result) and also with oscillator functions ($b = 1.7$ fm), respectively. The data are from Sakaguchi *et al.* [18] and Korshenninkov *et al.* [13], portrayed by the circles and squares, respectively. In the case of the differential cross section, the data to 80° are not sensitive enough to distinguish between the three results, although there may be a slight preference for the halo result at larger angles. This is in contrast to the analyses of proton scattering at lower energies which definitively show the halo [5,6].

For the analyzing power of ^{6}He, all calculations reproduce the data at forward angles. At larger angles, all models predict a positive analyzing power, while the data indicate an analyzing power that is flat and near zero. However, it is noteworthy that the data were obtained by binning over 10° in angle to obtain each datum [18], as shown in the figure. That binning may give rise to a problem in establishing the analyzing power at these angles: the averaging inherent in the binning, especially over such a large angular range may yield a smaller value in the analyzing power. This is especially critical as the analyzing power is a sensitive cancellation of terms in the scattering amplitude, normalized to the differential cross section. There is also an additional uncertainty of 19% in the scale of the measured analysing power [18]. As such, further experiments may be necessary to provide better data by which to evaluate the analyzing power.

The results for elastic scattering of ^{8}He ions from hydrogen are presented in Fig. 3, where the data portrayed are from

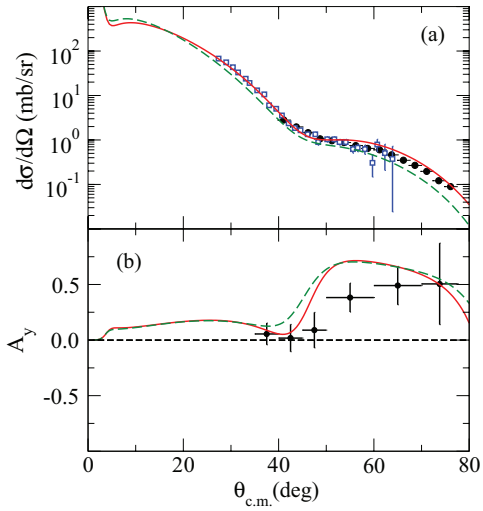

FIG. 3. (Color online) (a) Differential cross sections and (b) analyzing powers for the scattering of 71A MeV ^{8}He ions from Hydrogen. The WS no halo and halo results are portrayed by the solid and dashed lines, respectively.

Sakaguchi *et al.* [19] (circles) and Korshennikov *et al.* [13] (squares). In this case, the WS calculation uses the pertinent single particle wave functions with the correct single-nucleon binding energies for ^{8}He [1], the result of which is displayed by the solid line. In this case, the result is termed "no halo", and that result agrees well with the data. The "halo" result corresponds, somewhat arbitrarily, to the setting of those single-nucleon binding energies much lower, more in line with that of ^{6}He, as we had done previously [1]. The data show a preference for the no halo result, consistent with the description of ^{8}He nucleus as that having a neutron skin.

Unlike the analysis of the cross section data, the analysis of the analyzing power data show little difference between the two results, save for there being a preference again for the no-halo case. The data still have the problem of binning, as was the case for scattering from ^{6}He. There is better agreement with the data in this case. More data may be needed for both scatterings, however.

V. CONCLUSIONS

We have presented analyses of analyzing power data for the scattering of intermediate energy ^{6}He and ^{8}He ions from hydrogen. The g-folding approach, based on the use of multi-$\hbar\omega$ no-core shell model wave functions, with appropriate WS single-particle wave functions, gives agreement with both differential cross-section and analyzing power data. Central to this level of agreement is the constraint of the binding energy of the WS functions to the separation energy of the single nucleon from the target. This applies to both ^{6}He and ^{8}He, the former giving rise to an extensive neutron density, otherwise called the halo. The neutron skin in ^{8}He is also reproduced.

Given that the analyzing powers are very sensitive to the details of the interaction between the projectile and target, it is tempting to interpret the data as indicating new physics in describing that interaction. However, while the general shapes of the analyzing powers are reproduced by the calculations from the microscopic model, more data will be needed to make conclusive statements.

ACKNOWLEDGMENTS

We would like to thank S. Sakaguchi for useful discussions. S.K. acknowledges support of the National Research Foundation of South Africa.

[1] K. Amos, P. J. Dortmans, H. V. von Geramb, S. Karataglidis, and J. Raynal, Adv. Nucl. Phys. **25**, 275 (2000).
[2] J. Raynal, computer program DWBA98, NEA 1209/05, 1998.
[3] S. Karataglidis, P. G. Hansen, B. A. Brown, K. Amos, and P. J. Dortmans, Phys. Rev. Lett. **79**, 1447 (1997).
[4] S. Karataglidis, P. J. Dortmans, K. Amos, and C. Bennhold, Phys. Rev. C **61**, 024319 (2000).
[5] A. Lagoyannis *et al.*, Phys. Lett. B **518**, 27 (2001).
[6] S. Stepantsov *et al.*, Phys. Lett. B **542**, 35 (2002).
[7] P. K. Deb, K. Amos, S. Karataglidis, M. B. Chadwick, and D. G. Madland, Phys. Rev. Lett. **86**, 3248 (2001).
[8] S. Karataglidis, K. Amos, B. A. Brown, and P. K. Deb, Phys. Rev. C **65**, 044306 (2002).
[9] M. Hatano *et al.*, Eur. Phys. J. A **25**, 255 (2005).
[10] E. J. Stephenson, R. C. Johnson, and F. Sammarruca, Phys. Rev. C **71**, 014612 (2005).
[11] K. Amos, S. Karataglidis, and Y. J. Kim, Nucl. Phys. A **762**, 230 (2005).
[12] M. Dupuis, Ph.D. thesis, University of Bordeaux (unpublished, 2006); private communication.
[13] A. A. Korsheninnikov *et al.*, Nucl. Phys. A **617**, 45 (1997).
[14] D. C. Zheng, B. R. Barrett, J. P. Vary, W. C. Haxton, and C.-L. Song, Phys. Rev. C **52**, 2488 (1995).
[15] V. G. J. Stoks, R. A. M. Klomp, C. P. F. Terheggen, and J. J. de Swart, Phys. Rev. C **49**, 2950 (1994).
[16] D. J. Millener, J. W. Olness, E. K. Warburton, and S. S. Hanna, Phys. Rev. C **28**, 497 (1983).
[17] S. Karataglidis, Y. J. Kim, and K. Amos, Nucl. Phys. A **793**, 40 (2007).
[18] S. Sakaguchi *et al.*, Phys. Rev. C **84**, 024604 (2011).
[19] S. Sakaguchi *et al.*, Phys. Rev. C **87**, 021601(R) (2013).